FLASH Investigations Using Protons: Design of Delivery System, Preclinical Setup and Confirmation of FLASH Effect with Protons in Animal Systems

Authors: Zhang, Qixian, Cascio, Ethan, Li, Chengming, Yang, Qingyuan, Gerweck, Leo E., et al.

Source: Radiation Research, 194(6) : 656-664

Published By: Radiation Research Society

URL: https://doi.org/10.1667/RADE-20-00068.1

RADIATION RESEARCH **194**, 656–664 (2020)
0033-7587/20 $15.00

DOI: 10.1667/RADE-20-00068.1

FLASH Investigations Using Protons: Design of Delivery System, Preclinical Setup and Confirmation of FLASH Effect with Protons in Animal Systems

Qixian Zhang, Ethan Cascio, Chengming Li, Qingyuan Yang, Leo E. Gerweck, Peigen Huang, Bernard Gottschalk, Jacob Flanz and Jan Schuemann[1]

Department of Radiation Oncology, Massachusetts General Hospital and Harvard Medical School, Boston, Massachusetts

Zhang, Q., Cascio, E., Li, C., Yang, Q., Gerweck, L. E., Huang, P., Gottschalk, B., Flanz, J. and Schuemann, J. FLASH Investigations Using Protons: Design of Delivery System, Preclinical Setup and Confirmation of FLASH Effect with Protons in Animal Systems. *Radiat. Res.* 194, 656–664 (2020).

Extremely high-dose-rate irradiation, referred to as FLASH, has been shown to be less damaging to normal tissues than the same dose administrated at conventional dose rates. These results, typically seen at dose rates exceeding 40 Gy/s (or 2,400 Gy/min), have been widely reported in studies utilizing photon or electron radiation as well as in some proton radiation studies. Here, we report the development of a proton irradiation platform in a clinical proton facility and the dosimetry methods developed. The target is placed in the entry plateau region of a proton beam with a specifically designed double-scattering system. The energy after the double-scattering system is 227.5 MeV for protons that pass through only the first scatterer, and 225.5 MeV for those that also pass through the second scatterer. The double-scattering system was optimized to deliver a homogeneous dose distribution to a field size as large as possible while keeping the dose rate >100 Gy/s and not exceeding a cyclotron current of 300 nA. We were able to obtain a collimated pencil beam (1.6 × 1.2 cm² ellipse) at a dose rate of ~120 Gy/s. This beam was used for dose-response studies of partial abdominal irradiation of mice. First results indicate a potential tissue-sparing effect of FLASH.

INTRODUCTION

Radiation therapy is an effective treatment for primary solid cancers. Further improvement in therapeutic efficacy may be achieved by increasing the dose to tumors within the tolerance limits of surrounding normal tissues. Advanced radiotherapy technologies have increased precision and conformality of dose delivery, however, non-negligible side effects and resulting healthy tissue constraints impede further dose escalation. Renewed focus on the unique normal tissue-sparing benefits of FLASH radiotherapy has triggered great research interest in the phenomenon since 2014. Compared with conventional-dose-rate (CDR) irradiation, extreme-dose-rate photon or electron beams have been shown to spare normal tissues, such as brain (*1–4*), lung (*5*), and skin (*6*), without compromising tumor control (*5, 7*). To date, most experiments have been performed using photon and electron irradiations. These studies used beams generated by modified clinical linear accelerators (*8*), synchrotrons (*9*) or some prototype linacs (*10*). Recently, University of Pennsylvania researchers conducted whole-abdominal proton irradiation at a dose rate of 78 ± 9 Gy/s to test the protective effect of FLASH proton beam. Compared with conventional-dose-rate irradiation, the loss of proliferating intestinal crypt cells was significantly reduced by FLASH proton irradiation (*11*).

Before applying FLASH radiotherapy to the clinic, the mechanism underlying its normal tissue-sparing effect needs to be understood to determine its appropriate use and maximize its potential efficacy for clinical practice. It has been suggested that rapid oxygen consumption by FLASH pulses leads to oxygen depletion or instantaneous hypoxia and enhances radioresistance of normal tissues (*12*). In addition, it has been suggested that normal tissues may exhibit a greater capacity to eliminate radiation-induced reactive oxygen species than tumors (*13*). Experiments are ongoing to test these hypotheses.

Compared with photon therapy, proton therapy has a clinical advantage in dose conformity. Both passively scattered proton beams and scanning pencil beams allow the delivery of target doses with much lower integral dose compared to photon techniques (*14, 15*). Combining the advantageous dose distributions delivered to normal tissue by proton therapy with the potential normal tissue-sparing effect of FLASH may provide a new level of treatment

Editor's note. The online version of this article (DOI: https://doi.org/10.1667/RADE-20-00068.1) contains supplementary information that is available to all authorized users.

[1] Address for correspondence: Massachusetts General Hospital, Rm. 3206, 125 Nashua Street, Boston, MA, 02114; email: jschuemann@mgh.harvard.edu.

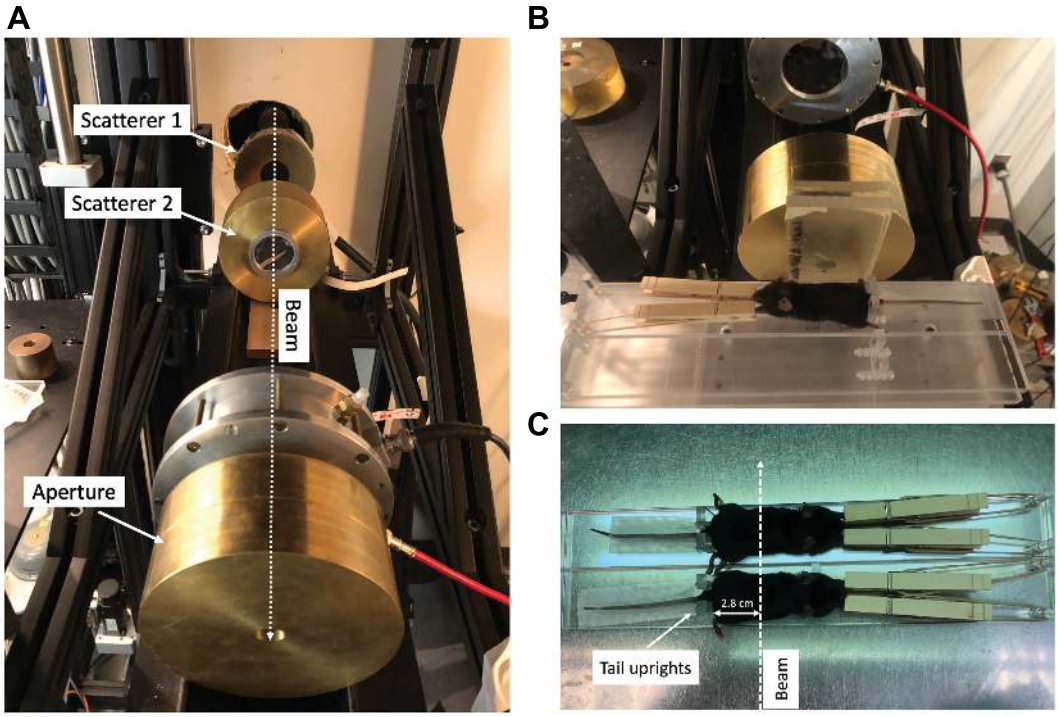

FIG 1. The experimental set-up enables irradiation of two mice at the same time. Mouse phantoms and Monte Carlo simulations are used to evaluate the dose. Panel A: The double-scattered system. Panels B and C: Mouse holders used for the reproducible immobilization. The beam can go through two parallel mice laterally.

optimization in radiation therapy, allowing for further dose escalation, which can improve tumor control, or alternatively reduced normal tissue toxicity, which is particularly important for long-term survivors.

In this article, the development of a FLASH proton platform using the experimental beamline of our existing clinical treatment facility is presented. The steps from initial design to preliminary results assessing the abdominal tissue-sparing capacity of extreme-dose-rate proton beams are shown.

MATERIALS AND METHODS

Design of a Proton Beam Delivery System for FLASH

Irradiations were performed at the Francis H. Burr Proton Therapy Center at Massachusetts General Hospital (Boston, MA). To avoid conflicts with clinical safety features that are defined for conventional dose rates, the experiments were designed for the experimental beamline. The experimental beamline is a parallel beamline coming from the cyclotron, passing the two gantry rooms and ending in the experimental room. We used a C230 isochronous cyclotron (Ion Beam Applications SA, Louvain-la-Neuve, Belgium) to accelerate the proton beam to 228.9 MeV. The cyclotron can provide a current of up to 300 nA in the standard operational mode, up to 450 nA with minor modifications and potentially higher currents with larger modifications such as changing the ion source. The proton beam is delivered with a radiofrequency of 106 MHz, resulting in bunches of ~3 ns with a spacing between the start of each bunch of 9.4 ns.

The protons are transported along the beamline to the experimental room, resulting in a spot size sigma of approximately 5 × 7.5 mm at maximum energy. To increase the size and to achieve a homogeneous radiation field across a 12 × 16 mm radiation field (95% falloff), a double-scattering system was designed consisting of a first scatterer with a 0.4064 mm (0.016″) lead foil placed 87.82 cm upstream of the surface of the first irradiation target/mouse, and a second scatter composed of a circular lead sheet of 0.8128 mm thickness (0.032″) with a radius of 1.65 mm placed on a thin mylar sheet positioned 52.29 cm upstream of the surface of the target. The design of the scattering system was optimized using an efficient Monte Carlo code[2] and subsequent TOPAS (*18*) Monte Carlo simulations to validate the accuracy of the selected settings.

An aperture was placed 8.56 cm upstream of the target surface with an oval shape with vertical and horizontal axis of 1.2 × 1.6 cm. The aperture consisted of 7.62 cm (3″) thick brass. The mice were irradiated on specifically designed holders of 4 cm width (Fig. 1B). Two mouse holders are placed in parallel on a fixed holder base (Fig. 1C) to allow simultaneous irradiation of two mice to reduce the required beamtime. Each position would have a specific dose level determined by the loss of dose between the two positions.

Dosimetry Validation

Dosimetric experiments were conducted to quantify the dose at extreme dose rates and evaluate beam flatness and the size of the radiation field with a combination of thin-gap parallel-plate ion chamber, thimble chamber, Faraday cup, Gafchromic™ film and Monte Carlo simulation.

The saturation of the thin-gap ion chamber was measured using a Faraday cup as baseline. We found that the thin-gap parallel-plate ion chamber had a recombination rate of less than 2% at maximum dose rate by comparing measured doses between the ion chamber and the Faraday cup for a wide range of dose rates from conventional dose rates of a few Gy/min to ~120 Gy/s with a 300-nA cyclotron current. A thimble chamber was used to test the dosimetry of the scattering apparatus at the center of each of the two mouse positions, in front of

[2] Developed by Bernie Gottschalk.

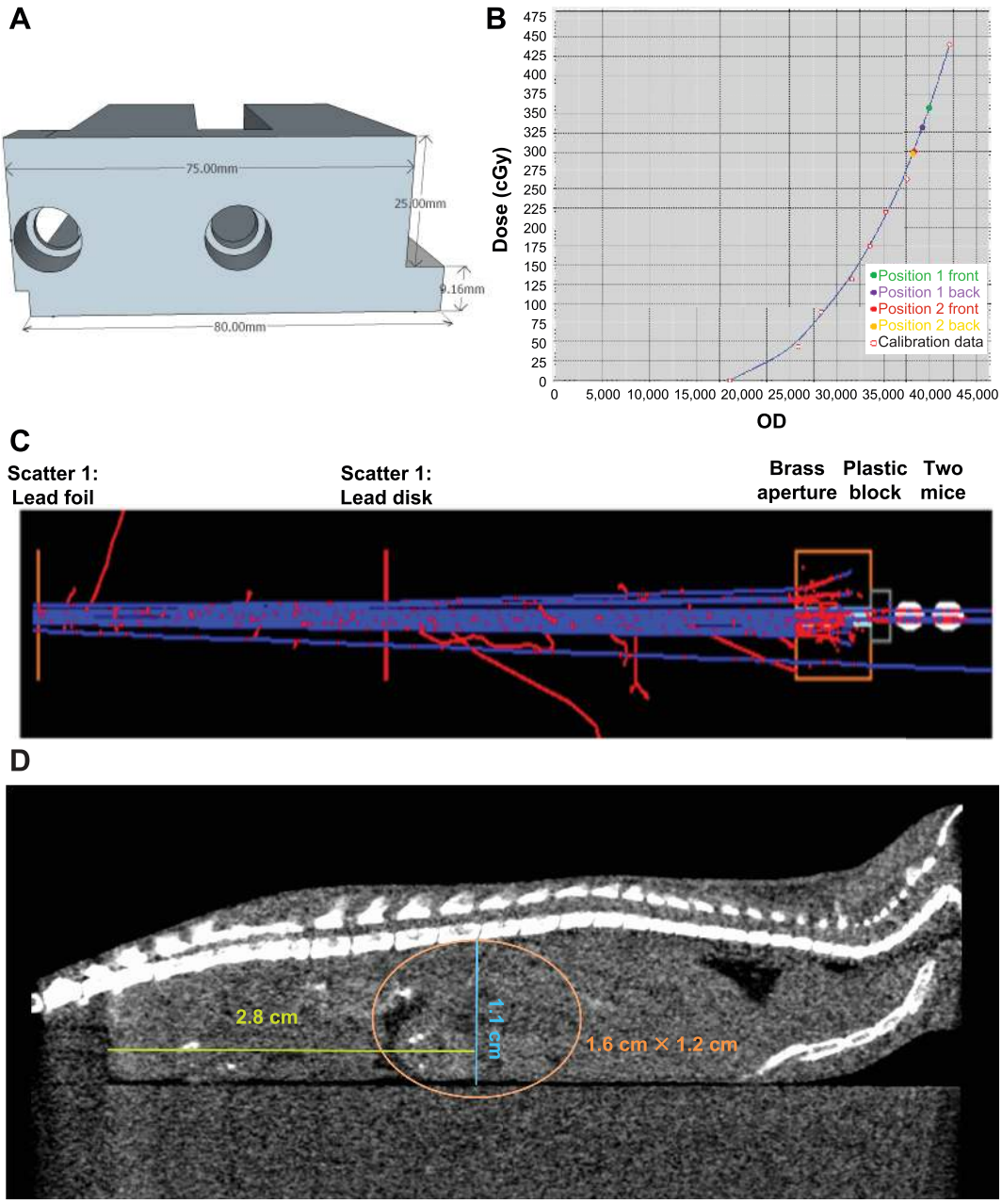

FIG 2. Dosimetry validation of the irradiation platform. Panel A: The diagram of the mouse phantom. Panel B: The dose distribution of the two mice verified by film measurements. Panel C: Schematic of the simulation setup. Panel D: The orange ellipse on the CT image indicates the radiation field. Panels E–G: The films at different depths of the phantom, 0 cm (panel E) and 3 cm (panel F), and the Monte Carlo simulation result (panel G) suggest a dramatic dose drop-off in the first 2 cm. Panel H: Vertical and horizontal dose profiles reconstructed from the 2D dose scanning at the target position.

the first mouse, in between the two mice, and at the back of the second mouse using a specially-built mouse phantom (Fig. 2A). The thimble chambers were operated only at low dose rates (<0.745 Gy/s) and for low doses (<3 Gy) as an additional test of the absolute doses at different positions along the beamline and for validation of the Monte Carlo simulations. Since the scattering behavior of protons should not change with dose rate, these measurements were used to calibrate dose to monitor unit conversions for different positions. Additionally, the doses were evaluated using EBT3 Gafchromic film at each surface of the two mouse phantoms (front and back) (Fig. 2B).

To measure dose profiles of the small beam spot with high accuracy, we designed a new 2D scanning device constructed from a 3D printer to monitor the flatness of small FLASH proton beams. The vertical and horizontal dose distribution was measured with a DFLR1600 diode providing a 1 × 1 mm^2 active area. The diode was attached to a specially-designed holder that was attached in the position of the 3D-printer nozzle carriage, which enabled us to scan the dose profile within a few seconds. Amplified diode signals were acquired using a Lecroy Wavepro 715Zi digital oscilloscope (Chestnut Ridge, NY) and then reconstructed to present the dose profiles (*16, 17*).

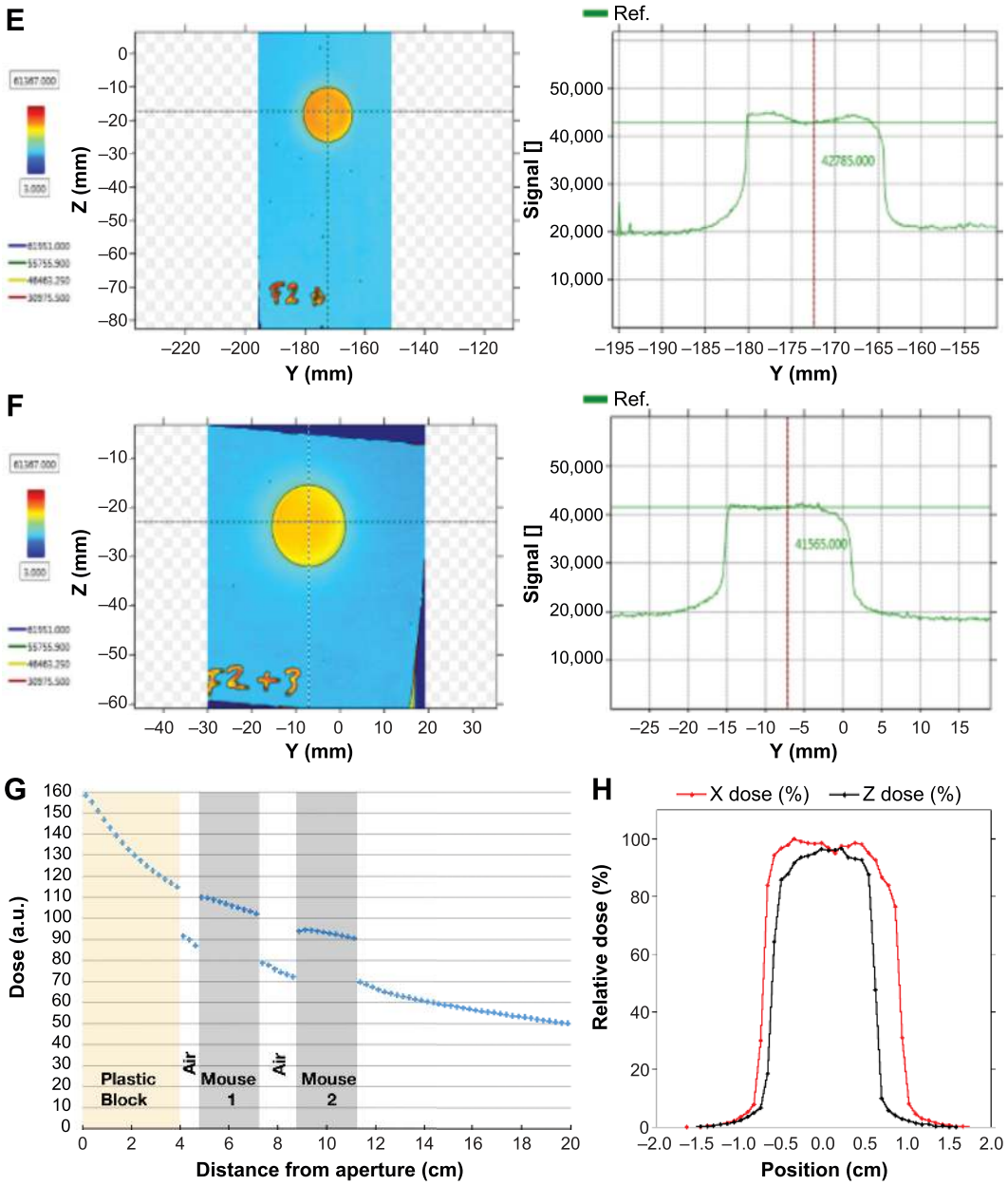

FIG 2. Continued.

Monte Carlo Simulations

Monte Carlo simulations were used for the design of the scattering system and evaluations of doses and dose distributions in the two mice. For the simulations we used the TOPAS Monte Carlo version 3.3 (*18*), which is based on Geant4 version 10.5.p01 (*19, 20*). A schematic view of the simulation setup is shown in Fig. 2C. The source was modeled as an emittance source with a Gaussian spread of 5 mm (7.5 mm) sigma in X (Y) and an energy at the beginning of the nozzle of 228.5 MeV. The mice are represented by water boxes of 2.5 cm thickness and dose distributions are scored by voxelizing the mouse phantom with 1 mm resolution in X and Y and a binning in Z of 0.5 mm. An additional scorer was used covering the central axis of the beamline. A TOPAS parameter file used for the simulations is included in the Supplementary Data (Text S1; https://doi.org/10.1667/RADE-20-00068.1.S1).

Animals

The experiments were conducted using 10-to-12-week-old female C57BL/6J mice (Jackson Laboratory, Bar Harbor, ME). C57BL/6 mice (n = 42) were randomly divided into eight cohorts (n = 6 animals in each 19 Gy group; n = 5 animals in the remaining dose groups plus one control group with n = 2) for FLASH or conventional-dose-rate proton irradiation (conventional group). All mice in this study were housed in micro-isolation cages (5 animals per cage), fed sterile pelleted chow, and given acidified sterile water *ad libitum*. All animal care and procedures were performed in accordance with the Public Health Service Policy on Humane Care of Laboratory Animals and approved by the Institutional Animal Care and Use Committee (IACUC) at Massachusetts General Hospital.

Imaging Procedures

Prior MRI and CT images were obtained from 4 and 3 mice, respectively, with mice in the constraining device to determine the optimal position for irradiations as well as the reproducibility and uncertainty in the setup. The positioning setup is composed of a plastic plate, a block with a gap for the tail and two columns (Supplementary Fig. S1; https://doi.org/10.1667/RADE-20-00068.1.S1). Each mouse was fixed on the plate using two clips pulling the front limbs with rubber bands tested to reduce stress and pain for the mice while providing reproducible setup accuracy and tape to constrain the tail such that the hip is fixed against the block. The maximal distance from the proximal boundary of the bladder to the fixed frame was found to be 2.0 cm based on MRI imaging. Thus, the caudal field border was set 2.0 cm away from the frame to exclude the bladder from the field. The orange ellipse in the CT image indicates the planned 1.6×1.2 cm^2 lateral radiation field (Fig. 2D). The maximal height of the radiation field was set to be 1.1 cm away from the surface of the mouse holder to protect the spinal cord. The mice were positioned in the entry region of the monoenergetic proton beam. This setup provided sufficient conformality within the field for two mice to be irradiated within the same beam.

Irradiation Procedures

The collimation of the proton pencil to the small target size resulted in a significant scattering component within the aperture. For the experiment reported here, we reduced the contribution of aperture scattering by placing 2 cm of polymethyl methacrylate plastic in front of the mice leaning against the aperture as the dose drop-off was much higher in the first 2 cm according to both film dosimetry (Fig. 2E and F) and Monte Carlo simulations (Fig. 2G). While a 2-cm plastic absorber was sufficient for single mouse experiments, in the future the amount of plastic will be increased to 4 cm for experiments with two mice in the beam to reduce inhomogeneous dose distribution in the mice and reduce the dose falloff between the mice. In that scenario, the aperture will be shifted upstream by 2 cm.

Our proton irradiation setup enabled us to deliver a dose to two mice at a time, with a reduction in dose of ~16% between the two mice and an acceptable enlargement of the field size. The radius of the dose profiles from Monte Carlo simulations (Supplementary Fig. S2; https://doi.org/10.1667/RADE-20-00068.1.S1) increased by approximately 3% from the center of the first mouse position to the center of the second mouse position. The 16% difference in dose can be used to irradiate two dose cohorts (e.g., 16 and 18.6 Gy) at the same time, significantly improving irradiation efficiency.

Prior to irradiation, each mouse was anesthetized with a mixture of ketamine (100 mg/kg) and xylazine (10 mg/kg) and restrained on the mouse holder. The beam profile and positioning enabled the irradiation of two mice at a time as indicated in Fig. 1A. All mice were irradiated in the entrance plateau region of the monoenergetic beam. Each FLASH procedure was completed within 180 ms using ~120 Gy/s proton beams. The sub-structure of our delivery time consisted of a pulsed beam from the cyclotron. A total of 21 C57Bl/6 mice were irradiated at FLASH dose rates. Each group received a dose ranging from 13 to 22 Gy in 3 Gy increments. The absolute dose and dose rate received by each mouse is shown in Supplementary Table S1 (https://doi.org/10.1667/RADE-20-00068.1.S1). In addition, a conventional cohort of C57Bl/6 mice ($n = 21$), received a conventional dose rates of 1.9 Gy/min to 4.5 Gy/min, keeping the irradiation time constant at approximately 5 min for doses between 13 and 22 Gy.

Histopathologic Examination

At day 90 postirradiation, intestinal tissues were collected from the control and irradiated surviving mice and fixed in 10% neutral buffered formalin. Then the Swiss-rolling (*21*) technique was implemented to prepare tissues for embedding. Briefly, intestine and colon were cut longitudinally and then rolled from the proximal end with the luminal side facing up. The tissues were pinned to keep the roll solid. After embedding in paraffin, the tissues were cut at 5-μm thickness, and routinely stained with hematoxylin and eosin (H&E). These sections enabled us to assess the histopathologic features of damage and repair after irradiation within the whole intestinal and colonic tissues.

Statistical Analysis

Statistical analysis was performed using the Graphpad Prism 7 software (La Jolla, CA) (*22*). Statistical evaluations were performed for the survival data and the weight loss. The comparison of weight loss between the FLASH and conventional groups was implemented using a *t* test. The log-rank test was used in the analysis of survival fractions. All data are presented as mean ± SEM, and $P < 0.05$ was considered to be statistically significant.

RESULTS

FLASH Proton Platform Setup and Dosimetry

The highest dose rate measured during the mouse irradiations was 137.88 Gy/s. We found that the delivered dose rate fluctuated between 106 Gy/s and 138 Gy/s during our first irradiations. The system became more stable over time, with much less fluctuations for the final set of mice (between 122 Gy/s and 128 Gy/s); see Supplementary Table S1 (https://doi.org/10.1667/RADE-20-00068.1.S1). In the future, FLASH experiments will be performed after the conventional-dose-rate irradiations to allow for the machine to warm up thereby reducing dose-rate fluctuations.

Reconstructed curves from the 2D dose scanning without aperture showed a field of 1.6×1.2 cm^2 at 90% of the maximum dose value (Fig. 2H). The beam covered approximately 65% of the volume of the abdomen.

Irradiation Outcome

Figure 3A and B shows the survival curves of the eight mouse groups. The mice were followed for 21 days. The first two mice reaching the defined end points were observed at day 6 after 22 Gy FLASH. All conventional and FLASH irradiated mice in the 19 Gy and 22 Gy groups died within 15 days. Compared to the 16 Gy conventional group (two survivors), the surviving fraction of C57BL/6 mice in the FLASH group with corresponding dose level was substantially higher (Fig. 3C, $P = 0.049$). All mice irradiated with 13 Gy survived. At day 9 postirradiation, the weight loss of 16 Gy conventional irradiated C57BL/6 mice was most pronounced, and significantly differed from the FLASH group in both absolute weight value (Fig. 4A) and percentage weight loss (Fig. 4B), but the difference was significant only at day 9. Two mice survived in the 16 Gy conventional group and their weight recovered completely at day 12 postirradiation after up to 11.8% weight loss. Less time was needed for the weight of the 16 Gy FLASH irradiated C57BL/6 mice to recover their initial weight. The initial weight of the mice can be found in Supplementary Table S1 (https://doi.org/10.1667/RADE-20-00068.1.S1).

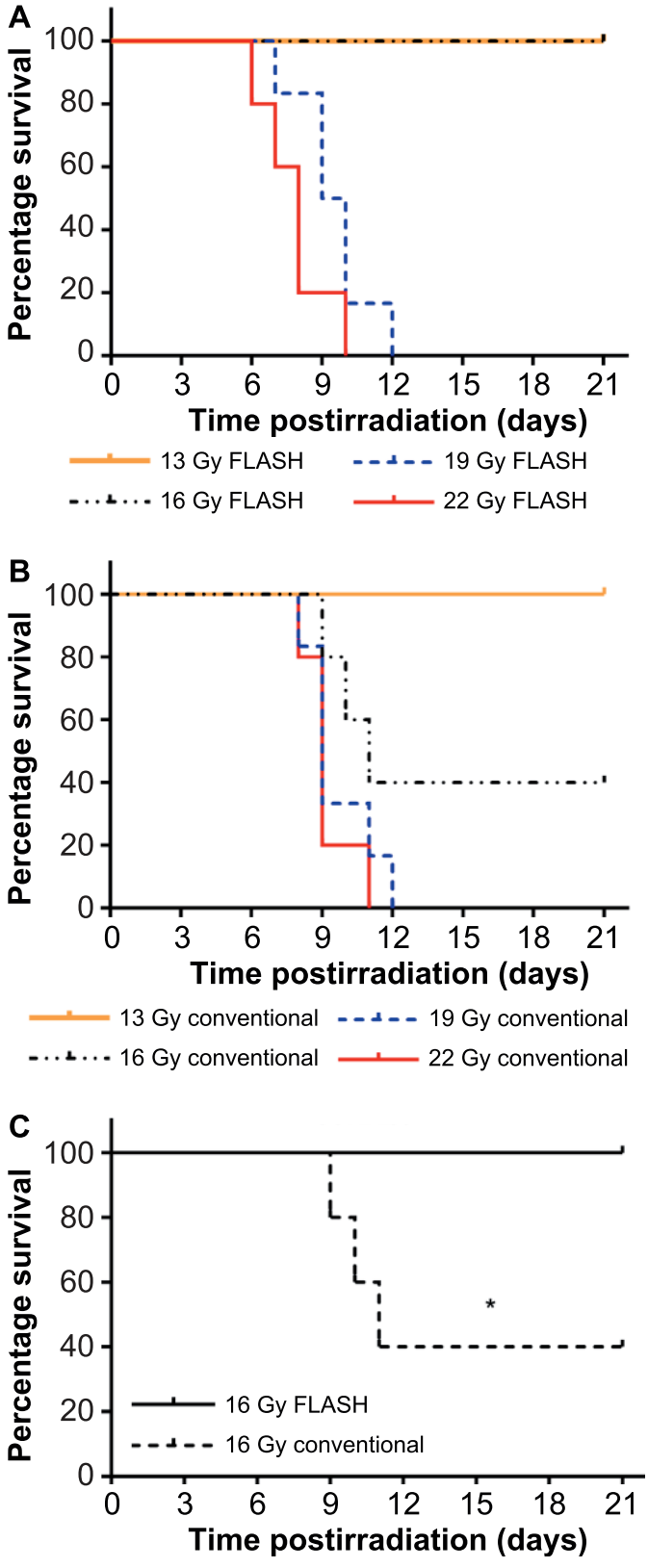

FIG 3. Survival curves of the FLASH (panel A) and conventional-dose-rate (panel B) irradiation groups. Panel C: The log-rank test result shows that FLASH irradiation causes less damage to the mice after partial-abdominal irradiation (n = 5 mice/group). *$P < 0.05$, compared to the conventional group.

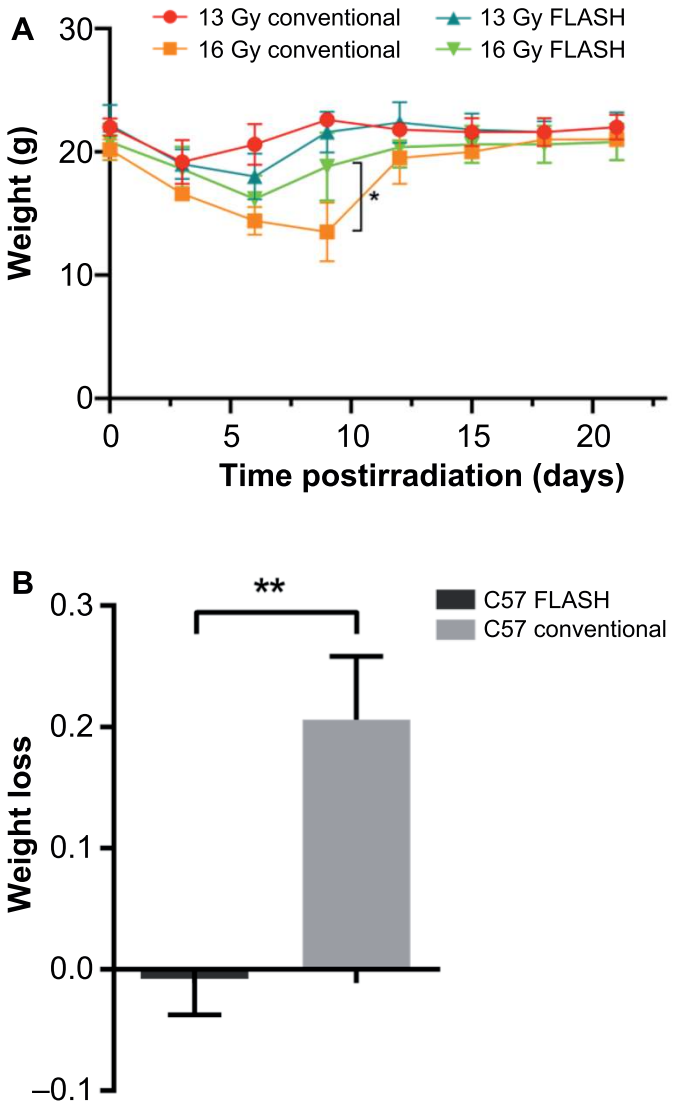

FIG 4. At day 9 after 16 Gy irradiation, the FLASH group shows higher absolute weight value (panel A) and less weight loss (panel B) (n = 5 mice/group). *$P < 0.05$, **$P < 0.01$, compared to the conventional group.

Late Intestinal Effect

Nonirradiated mice exhibited no inflammatory characteristics (Fig. 5A and B). Several layers of the intestinal rolls from the 16 Gy FLASH (Fig. 5C and D) and conventional dose-rate (Fig. 5E and F) irradiated mice showed collagen deposition, hyperplastic submucosa and muscularis as well as an infiltration of inflammatory cells. A necrotic lesion was observed in one mouse in the conventional group (Fig. S3; https://doi.org/10.1667/RADE-20-00068.1.S1). Overall, the submucosa and muscle layer in the FLASH group indicated improved repair (thinner layer); however, as only two mice in the 16 Gy conventional group survived, the sample size was not suitable for conducting statistical analysis to assess the late effect difference among these groups.

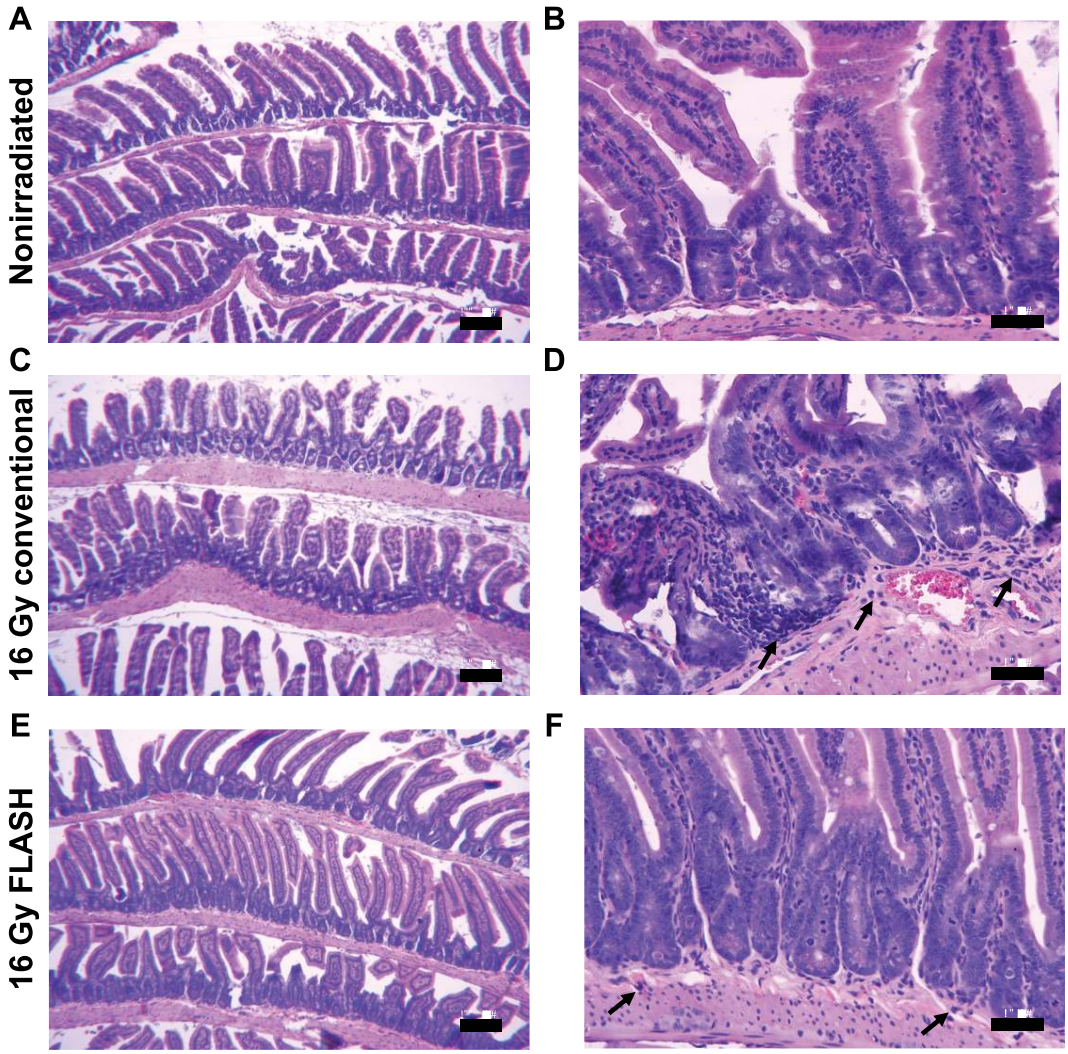

FIG 5. Images from H&E stains of the intestinal tissues from nonirradiated mice (panels A and B), FLASH proton irradiated mice (panels C and D) and conventional dose-rate proton irradiated mice (panels E and F) at day 90 postirradiation. Infiltrating inflammatory cells (arrows), thickening of the submucosa and muscularis, and chronic inflammatory cell infiltration (arrows) were observed in both of 16 Gy FLASH and conventional irradiated small intestine.

DISCUSSION

In this proof-of-principle study, we established a reliable FLASH proton platform for small animal experiments with only minor modification of our clinical facility. Creative usage of the 2D dosimetry scanning system improved the efficiency and precision of measuring the dose profiles. A dose rate of up to 138 Gy/s was achieved using a double-scattering system for irradiating mice at the entrance plateau region of a single pristine Bragg peak. A satisfactory dose distribution was obtained, and doses and dose rates were verified using a combination of radiochromic film, Monte Carlo simulation, Faraday cup, and two different ion chamber measurements. Patriarca *et al*. also built a FLASH proton irradiation set-up for small animal experiments utilizing the spread-out Bragg peak (SOBP) (*23*); however, their design aimed at much lower dose rates in the order of 40 Gy/s, and included a ridge filter to obtain a spread-out Bragg peak for treatment. The FLASH proton radiation system at the University of Pennsylvania was reported to be able to deliver a proton beam with a dose rate of 60–100 Gy/s and a FLASH effect on intestine was observed (*11*).

Our results demonstrate that the FLASH effect on fast-responding abdominal tissues can be generated by a single dose of FLASH proton radiation. C57BL/6 mice showed notably (while statistically limited) better tolerance to FLASH protons than to equivalent doses for conventional dose rates. Preliminary results from Loo *et al*. showed a significant survival difference between conventional-dose-rate (0.05 Gy/s) and FLASH groups. The LD_{50} was 16.6 and 18.3 Gy for mice after 70 and 210 Gy/s electron abdominal

irradiation, respectively (*24*). Preserved gut function, reduced cell death in crypts and fewer γ-H2AX foci were observed after FLASH electron irradiation (*25*). In our research, approximately 120 Gy/s partial abdominal FLASH proton irradiation decreased body weight loss and mortality rate at 16 Gy. It should be noted, however, that the current experiments were pure proof-of-concept experiments with low statistical power. A different outcome of one mouse in either cohort would result in non-significant results.

The mechanisms responsible for the FLASH tissue-sparing effect are not yet well understood. Extremely rapid depletion of tissue oxygen by a sufficiently high dose administered within milliseconds is a potential explanation for the FLASH effect. The first quantified demonstration of oxygen depletion by high-dose-rate irradiation was conducted in bacteria in 1959 (*26*). Similar studies were subsequently performed in mammalian cells *in vitro* (*27, 28*). In 1971, Hornsey *et al*. found that the protective effect of high-dose-rate electron irradiation in mice could be reduced by breathing oxygen-free nitrogen for 25 s (*29*). At a high dose rate, no effect was observed on anoxic rat feet skin (*30*). The results of a later study also suggested that the protective effect of extreme-dose-rate proton irradiation on skin was linked to oxygen consumption (*31*). Additionally, high-concentration oxygen also reduced or eliminated the neurocognitive benefits of 10 Gy FLASH dose (*1*). Significant tissue-sparing effects after 10 Gy irradiations at high dose rates will likely be observed when the oxygen tension is 3–5 mmHg (*32*). If oxygen depletion is the dominant factor, the dose at which the FLASH effect can be observed will depend not only on the initial oxygen concentration but also on the delivered dose and the dose rate.

Another potential hypothesis involves the sparing of circulating lymphocytes. The immune system responds to the unbalanced tissue environment after ionizing radiation exposure. Lymphocytes are recruited to the damaged sites and modulate inflammatory reactions (*33, 34*). High-dose-rate irradiations reduce the volume of blood and the proportion of circulating lymphocytes that experience radiation damage, which may play a role in the FLASH effect. Genome-wide microarray analysis of mice receiving whole-thorax irradiation suggests the involvement of immune modulation pathways, such as dendritic cell maturation, PKC signaling in lymphocytes, TH1 pathway modulation and calcium-induced T-lymphocyte apoptosis, in the FLASH effect (*35*). However, Venkatesulu *et al*. reported that 35 Gy/s cardiac or splenic irradiation depleted more lymphocytes than conventional-dose-rate irradiation (*36*).

The ''FLASH mode'' is typically defined by the mean dose rate of the whole irradiation procedure. However, parameters, such as intra-pulse dose rate, pulse frequency and fraction pattern of the total dose, should also be carefully considered. Judging from previously reported studies, both single-pulse and multiple-pulse rays are able to trigger the FLASH effect (*1, 3*). In our study, a train of pulses were delivered to the FLASH cohorts, resulting in a relatively constant dose rate experienced at the cell scale. If our preliminary results can be reproduced with higher statistical experiments, we can assume that the dose can be delivered with different pulse structures as long as the average dose rate is high enough.

CONCLUSION

We demonstrated the setup of a FLASH platform using an existing proton infrastructure, allowing us to investigate the FLASH effect of protons on different tissues and organs. The results for our first, low statistical experiments indicate that extreme-dose-rate proton beams were less harmful to the normal gastrointestinal tract than the same doses delivered at normal dose rates.

SUPPLEMENTARY INFORMATION

Table S1. The initial body weight as well as the absolute dose and dose rate received by each mouse.

Fig. S1. The specifically designed holder for mouse irradiation.

Fig. S2. The Monte Carlo simulation result indicated ~16% dose difference between two mice.

Fig. S3. Tissue necrosis was observed after conventional dose rate proton irradiation.

Text S1. The TOPAS parameter file that is used for the simulations.

ACKNOWLEDGMENTS

We thank Iris Yuwen Zhou and Eric McDonald for helping us with the animal imaging. This study was supported by the Damon Runyon-Rachleff Innovation Award (no. DRR 57-19). We also thank the MGH Radiation Oncology Machine Shop for their help and support.

Received: March 3, 2020; accepted: August 14, 2020; published online: September 29, 2020

REFERENCES

1. Montay-Gruel P, Acharya MM, Petersson K, Alikhani L, Yakkala C, Allen BD, et al. Long-term neurocognitive benefits of FLASH radiotherapy driven by reduced reactive oxygen species. Proc Natl Acad Sci U S A 2019; 116:10943–51.
2. Montay-Gruel P, Bouchet A, Jaccard M, Patin D, Serduc R, Aim W, et al. X-rays can trigger the FLASH effect: Ultra-high dose-rate synchrotron light source prevents normal brain injury after whole brain irradiation in mice. Radiother Oncol 2018; 129:582–88.
3. Simmons DA, Lartey FM, Schuler E, Rafat M, King G, Kim A, et al. Reduced cognitive deficits after FLASH irradiation of whole mouse brain are associated with less hippocampal dendritic spine loss and neuroinflammation. Radiother Oncol 2019; 139:4–10.
4. Montay-Gruel P, Petersson K, Jaccard M, Boivin G, Germond J-F, Petit B, et al. Irradiation in a Flash: Unique sparing of memory in mice after whole brain irradiation with dose rates above 100 Gy/s. Radiother Oncol 2017; 124:365–69.
5. Favaudon V, Caplier L, Monceau V, Pouzoulet F, Sayarath M, Fouillade C, et al. Ultrahigh dose-rate FLASH irradiation increases

the differential response between normal and tumor tissue in mice. Sci Transl Med 2014; 6:245ra93.

6. Vozenin MC, De Fornel P, Petersson K, Favaudon V, Jaccard M, Germond JF, et al. The advantage of FLASH radiotherapy confirmed in mini-pig and cat-cancer patients. Clin Cancer Res 2019; 25:35–42.
7. Vozenin MC, Hendry JH, Limoli CL. Biological benefits of ultra-high dose rate FLASH radiotherapy: Sleeping beauty awoken. Clin Oncol (R Coll Radiol) 2019; 31:407–15.
8. Lempart M, Blad B, Adrian G, Back S, Knoos T, Ceberg C, et al. Modifying a clinical linear accelerator for delivery of ultra-high dose rate irradiation. Radiother Oncol 2019; 139:40–5.
9. Smyth LML, Donoghue JF, Ventura JA, Livingstone J, Bailey T, Day LRJ, et al. Comparative toxicity of synchrotron and conventional radiation therapy based on total and partial body irradiation in a murine model. Sci Rep 2018; 8:12044.
10. Jaccard M, Duran MT, Petersson K, Germond JF, Liger P, Vozenin MC, et al. High dose-per-pulse electron beam dosimetry: Commissioning of the Oriatron eRT6 prototype linear accelerator for preclinical use. Med Phys 2018; 45:863–74.
11. Diffenderfer ES, Verginadis, II, Kim MM, Shoniyozov K, Velalopoulou A, Goia D, et al. Design, implementation, and in vivo validation of a novel proton FLASH radiation therapy system. Int J Radiat Oncol Biol Phys 2020; 106:440–8.
12. Wilson P, Jones B, Yokoi T, Hill M, Vojnovic B. Revisiting the ultra-high dose rate effect: implications for charged particle radiotherapy using protons and light ions. Br J Radiol 2012; 85:e933–9.
13. Spitz DR, Buettner GR, Petronek MS, St-Aubin JJ, Flynn RT, Waldron TJ, et al. An integrated physico-chemical approach for explaining the differential impact of FLASH versus conventional dose rate irradiation on cancer and normal tissue responses. Radiother Oncol 2019; 139:23–7.
14. Chang JY, Zhang X, Wang X, Kang Y, Riley B, Bilton S, et al. Significant reduction of normal tissue dose by proton radiotherapy compared with three-dimensional conformal or intensity-modulated radiation therapy in Stage I or Stage III non-small-cell lung cancer. Int J Radiat Oncol Biol Phys 2006; 65:1087–96.
15. Lomax A. Intensity modulation methods for proton radiotherapy. Phys Med Biol 1999; 44:185–205.
16. Cascio EW, Bentefour EH. The use of diodes as dose and fluence probes in the experimental beamline at the Francis H. Burr Proton Therapy Center. 2011 IEEE Radiation Effects Data Workshop; 2011; 1–6.
17. Cascio EW, Gottschalk B. Using a 3D printer for 2D beam profile measurements in proton radiotherapy. arXiv 2019; 1908.03763.
18. Perl J, Shin J, Schumann J, Faddegon B, Paganetti H. TOPAS: an innovative proton Monte Carlo platform for research and clinical applications. Med Phys 2012; 39:6818–37.
19. Agostinelli S, Allison J, Amako K, Apostolakis J, Araujo H, Arce P, et al. GEANT4–a simulation toolkit. Nucl Instrum Methods Phys Res A 2003; 506:250–303.
20. Allison J, Amako K, Apostolakis J, Arce P, Asai M, Aso T, et al. Recent developments in Geant4. Nucl Instrum Methods Phys Res A 2016; 835:186–225.
21. Bialkowska AB, Ghaleb AM, Nandan MO, Yang VW. Improved Swiss-rolling technique for intestinal tissue preparation for immunohistochemical and immunofluorescent analyses. J Vis Exp 2016; 113:54161.
22. Adusumilli P, Konatam ML, Gundeti S, Bala S, Maddali LS. Treatment challenges and survival analysis of human epidermal growth factor receptor 2-positive breast cancer in real world. Indian J Med Paediatr Oncol 2017; 38:22–7.
23. Patriarca A, Fouillade C, Auger M, Martin F, Pouzoulet F, Nauraye C, et al. Experimental set-up for FLASH proton irradiation of small animals using a clinical system. Int J Radiat Oncol Biol Phys 2018; 102:619–26.
24. Loo BW, Schuler E, Lartey FM, Rafat M, King GJ, Trovati S, et al. (P003) delivery of ultra-rapid Flash radiation therapy and demonstration of normal tissue sparing after abdominal irradiation of mice. Int J Radiat Oncol Biol Phys 2017; 98:E16.
25. Levy K, Natarajan S, Wang J, Chow S, Eggold J, Loo P, et al. FLASH irradiation enhances the therapeutic index of abdominal radiotherapy in mice. bioRxiv 2019.
26. Dewey DL, Boag JW. Modification of the oxygen effect when bacteria are given large pulses of radiation. Nature 1959; 183:1450–1.
27. Berry RJ, Hall EJ, Forster DW, Storr TH, Goodman MJ. Survival of mammalian cells exposed to x rays at ultra-high dose-rates. Br J Radiol 1969; 42:102–7.
28. Berry RJ, Stedeford JB. Reproductive survival of mammalian cells after irradiation at ultra-high dose-rates: further observations and their importance for radiotherapy. Br J Radiol 1972; 45:171–7.
29. Hornsey S, Bewley DK. Hypoxia in mouse intestine induced by electron irradiation at high dose-rates. Int J Radiat Biol Relat Stud Phys Chem Med 1971; 19:479–83.
30. Field SB, Bewley DK. Effects of dose-rate on the radiation response of rat skin. Int J Radiat Biol Relat Stud Phys Chem Med 1974; 26:259–67.
31. Kozin S, Zolotov V, Ponomareva N. Hypoxic proton radiotherapy of solid Ehrlich tumors with different dose magnitudes. (Article in Russian). Meditsinskaia Radiologiia 1984 ;29:27–33.
32. Pratx G, Kapp DS. Ultra-high-dose-rate FLASH irradiation may spare hypoxic stem cell niches in normal tissues. Int J Radiat Oncol Biol Phys 2019; 105:190–2.
33. Bessout R, Demarquay C, Moussa L, Rene A, Doix B, Benderitter M, et al. TH17 predominant T-cell responses in radiation-induced bowel disease are modulated by treatment with adipose-derived mesenchymal stromal cells. J Pathol 2015; 237:435–46.
34. Paun A, Kunwar A, Haston CK. Acute adaptive immune response correlates with late radiation-induced pulmonary fibrosis in mice. Radiat Oncol 2015; 10:45.
35. Girdhani S, Abel E, Katsis A, Rodriquez A, Senapati S, KuVillanueva A, et al. Abstract LB-280: FLASH: A novel paradigm changing tumor irradiation platform that enhances therapeutic ratio by reducing normal tissue toxicity and activating immune pathways. Cancer Res 2019; 79:LB-280.
36. Venkatesulu BP, Sharma A, Pollard-Larkin JM, Sadagopan R, Symons J, Neri S, et al. Ultra high dose rate (35 Gy/sec) radiation does not spare the normal tissue in cardiac and splenic models of lymphopenia and gastrointestinal syndrome. Sci Rep 2019; 9:17180.